Journal of Power Sources 266 (2014) 186–192

Contents lists available at ScienceDirect

Journal of Power Sources

journal homepage: www.elsevier.com/locate/jpowsour

Alkaline stable C2-substituted imidazolium-based cross-linked anion exchange membranes for alkaline fuel cell applications

Bencai Lin [a,b], Fuqiang Chu [a], Yurong Ren [a], Baoping Jia [a], Ningyi Yuan [a,b], Hui Shang [a], Tianying Feng [a], Yuanyuan Zhu [a], Jianning Ding [a,b,*]

[a] Jiangsu Key Laboratory for Solar Cell Materials and Technology, School of Materials Science and Engineering, Changzhou University, Changzhou, 213164 Jiangsu, China
[b] Jiangsu Collaborative Innovation Center of Photovolatic Science and Engineering, Changzhou, 213164 Jiangsu, China

HIGHLIGHTS

- C2-substituted imidazolium salt was synthesized and used both as crosslinker and hydrophilic phase.
- The imidazolium-based AEMs show the conductivity up to 2.0×10^{-2} S cm^{-1} at 90 °C.
- The imidazolium-based AEMs show good chemical stability in 1 M KOH solution.

ARTICLE INFO

Article history:
Received 27 February 2014
Received in revised form
30 April 2014
Accepted 2 May 2014
Available online 14 May 2014

Keywords:
Alkaline fuel cell
Anion exchange membranes
Imidazolium salts
Alkaline stability

ABSTRACT

Novel C2-substituted imidazolium-based cross-linked anion exchange membranes (AEMs) are prepared via irradiation with ultraviolet light cross-linking of styrene, acrylonitrile and 1,3-diallyl-2-methyl imidazolium bromine ([DAMIm][Br]), and followed by anion exchange with hydroxide ions. [DAMIm][Br] is synthesized and used both as crosslinker and hydrophilic phase. The ionic conductivity of the AEMs increases with increasing [DAMIm][Br] content due to the hydrophilic regions and the continuous hydrophilic polymeric networks formed in the membranes. The imidazolium-based cross-linked AEMs show excellent thermal stabilities, and the membrane which containing 30% mass fraction of [DAMIm][Br] shows ionic conductivity up to 2.0×10^{-2} S cm^{-1} and good long-term chemical stability in 1 M KOH solution. The results of this study suggest that the C2-substituted imidazolium-based cross-linked AEMs have good perspectives for alkaline fuel cell applications.

1. Introduction

Fuel cells have been recognized as one of the most promising power generation technologies that could provide clean and efficient energy for stationary, transportation, and portable electronics [1–3]. Among all kinds of fuel cells, proton exchange membrane fuel cells (PEMFCs) attracted much attentions due to their high power density, high energy-conversion efficiencies, low starting temperature, and ease of handling [4,5]. Nafion® perfluorosulfonic acid membranes, the most established and state-of-the-art proton exchange membranes (PEMs) used in PEMFCs, have high proton conductivities, good mechanical properties and excellent chemical stability [6,7]. However, the application of Nafion in PEMFCs is limited by their high production cost, environmental incompatibility of the perfluorinated materials, high gas permeability and insufficient thermomechanical properties above 80 °C [8,9]. In addition, the dependence of platinum catalysts of PEMFCs is an important consideration because of the high cost and the limited platinum resource in nature [10–12].

To solve these problems mentioned above, recently, great interests have been evoked on alkaline anion exchange membrane fuel cells (AEMFCs) which are a type of fuel cells using anion exchange membrane (AEM) instead of PEM as electrolyte. Compared with PEMFCs, the high pH operation of AEMFCs could both enhance the electrokinetics and reduce CO poisoning. In addition, the basic conditions of AEMFCs enable the use of non-precious metal catalysts (such as nickel and silver) instead of platinum catalysts [10,11],

* Corresponding author. Jiangsu Key Laboratory for Solar Cell Materials and Technology, School of Materials Science and Engineering, Changzhou University, Changzhou, 213164 Jiangsu, China. Tel./fax: +86 519 86450008.
E-mail addresses: cfq@cczu.edu.cn (F. Chu), nyyuan@cczu.edu.cn, nyyuan660211@163.com (N. Yuan), dingjn@cczu.edu.cn, dingjianning@tsinghua.org.cn (J. Ding).

http://dx.doi.org/10.1016/j.jpowsour.2014.05.003
0378-7753/

which dramatically lowers the cost of fuel cells. The advantages mentioned above make the AEMFC technology financially and technically doable.

As the core component of AEMFCs, AEMs have attracted much attentions. An excellent AEM for an AEMFC must have good chemical and thermal stability, sufficient mechanical strength, and high ionic conductivity. In the past several years, the AEMs containing quaternary ammonium cationic groups have been extensively studied [13–16]. They are commonly prepared by attachment of chloromethyl groups to polymer backbones and followed by quaternization to form ammonium salts. However, it has been demonstrated that quaternary ammonium-based AEMs are unstable in alkaline medium, especially at elevated temperatures [17,18]. Since the chemical stability of an AEM is strongly dependent on the nature of the cations, cations such as guanidinium cations [19–21], quaternary phosphonium cations [22–25], imidazolium cations [26–36] and benzimidazolium cations [37–40] other than quaternary ammonium cation groups based polymers have been recently extensively studied. Among the different kinds of AEMs, imidazolium-based AEMs have attracted much attention. Fang et al. [29] reported an imidazolium-based AEMs which prepared via free radical copolymerization and solution-casting method. After treatment with 10 M NaOH solution at 60 °C for 120 h, the conductivity of the membranes showed no significant change, which indicated the good chemical stability of the imidazolium-based AEMs. Yan et al. [33] reported a cross-linked imidazolium-based AEM which displays an excellent chemical stability up to 400 h in high pH solution without obvious loss of ion conductivity and mechanical properties. Though imidazolium cations show relatively higher chemical stability than ammonium cations in a wide range of alkaline condition, degradation was observed for imidazolium-based AEMs under vigorous conditions (such as dry conditions, higher temperature and alkaline concentrations) in our previous work [41]. These results suggest that imidazolium cations have considerable chemical stability in alkaline condition, but it still needs to be improved. The protection of cationic groups by steric hindrance and/or mesomeric stabilization might be a prospect way to enhance the chemical stability of cations. In our previous work, we found that C2-substituted imidazolium salts showed much more chemical stability than C2-unsubstituted imidazolium salt under alkaline condition at elevated temperature, and the compound with methyl at C2 position of imidazole ring (3-ethyl-1,2-dimethyl imidazolium bromine) showed the best alkaline stability in the four kinds of imidazolium salts [41].

More recently, Hickner's study showed that the main chain backbone structure of the polymers significantly influenced on the alkaline stability of the quaternary ammonium cations [42]. Their results indicated that the quaternary ammonium cations on vinyl polymer (QA-PS) have much more alkaline stability than that on main chain type aromatic polymers. However, vinyl polymer-based membranes generally have poor mechanical properties, especially when hydrated [42]. Thus, strategies to reinforce the mechanical properties of functionalized vinyl polymer-based AEMs are required. Chemical cross-linking is a feasible and effective method for improving the mechanical properties of membranes. Yan et al. synthesized an imidazolium-based cross-linked AEMs, and divinylbenzene (DVB) used as the crosslinker [33]. The mechanical properties of membranes increased with the increment of DVB content. However, the conductivity of the membranes decreased with increasing of DVB content because of DVB shows no ionic conductivity.

In the present work, a cross-linked vinyl polymer-based AEMs were synthesized and characterized. 1,3-Diallyl-2-methyl imidazolium bromine ([DAMIm][Br]) was synthesized and used both as crosslinker and hydrophilic phase. The properties of the membranes, such as water uptake, swelling degree, thermal stability, mechanical properties, ion exchange capacity (IEC), hydroxide ion conductivity and chemical stability were investigated.

2. Experimental

2.1. Materials

Styrene, acrylonitrile, ethyl ether, ethyl acetate, acetonitrile, chloroform, potassium hydroxide, anhydrous $MgSO_4$, sodium hydroxide and hydrochloric acid were purchased from Aladdin (Shanghai). 2-Methylimidazole, 3-bromo-1-propene and benzoin ethyl ether were purchased from Alfa Aesar. All of the vinyl monomers were made inhibitor-free by passing the liquid through a column filled with base Al_2O_3. Distilled deionized water was used for all experiments.

2.2. Synthesis of 1-allyl-2-methylimidazole

1-Allyl-2-methylimidazole was synthesized as follows: a mixture containing 2-methylimidazole 4.10 g (0.05 mol), 3-bromo-1-propene 6.05 g (0.05 mol), and 5.61 g (0.10 mol) KOH in acetonitrile (40 mL) was stirred at room temperature for 4 h under an argon atmosphere. The solvent was removed under dynamic vacuum, and the crude product was extracted with $CHCl_3$ three times. The combined organic phase was washed with distilled water and dried over anhydrous $MgSO_4$, and the solvent was removed under vacuum. The resultant yellow oil was dried in dynamic vacuum at room temperature. ^{1}H NMR (400 MHz, $CDCl_3$): δ: 6.87–6.89 (d, 1H), 6.76–6.78 (d, 1H), 5.82–5.90 (m, 1H), 5.16–5.19 (d, 2H), 4.92–4.96 (d, 1H), 4.39–4.41 (m, 2H), 2.30 (s, 3H).

2.3. Synthesis of 1,3-diallyl-2-methyl imidazolium bromine ([DAMIm][Br])

[DAMIm][Br] was synthesized by stirring the mixture of 1-allyl-2-methylimidazole with an equivalent molar amount of 3-bromo-1-propene at room temperature under nitrogen atmosphere. The resultant viscous oil was washed with ethyl ether three times and then dried in dynamic vacuum at room temperature for 24 h. ^{1}H NMR (400 MHz, D_2O): 7.35 (s, 2H), 5.90–6.00 (m, 2H), 5.32–5.34 (d, 2H), 5.09–5.14 (d, 2H), 4.71–4.73 (d, 4H), 2.52 (s, 3H).

2.4. Preparation of cross-linked composite membranes

A mixture of styrene/acrylonitrile (1:3 weight ratio, 90–70 wt%), [DAMIm][Br] (10–30 wt%), and benzoin ethyl ether (photo-initiator 1 wt% to the formulation based on the weight of monomer) was stirred and ultrasonicated to obtain a homogeneous solution, which was then cast into a glass mold and photo-cross-linked by irradiation with UV light of 250 nm wavelength in a glass mold for 30 min at room temperature. The resultant composite membranes were immersed in a N_2 saturated 1 M KOH solution at 60 °C for 24 h to convert the membrane from Br^- to OH^- form [43]. Then the converted membranes were immersed in a N_2 saturated deionized water and washed with N_2 saturated deionized water until the pH of residual water was neutral.

2.5. Characterization

^{1}H NMR spectra were recorded on a Varian 400 MHz spectrometer. Fourier transform infrared (FT-IR) spectra of the membranes were recorded on a Varian CP-3800 spectrometer in the range of 4000–400 cm^{-1}. Thermal analysis was carried out by Universal Analysis 2000 thermogravimetric analyzer (TGA). Samples were heated from 30 to 600 °C at a heating rate of 10 °C min^{-1}

under a nitrogen flow. The tensile properties of membranes were measured by using an Instron 3365 at room temperature at a crosshead speed of 5 mm min^{-1}. Scanning electron microscopy (SEM) images were taken with a Philips XL 30 FEG microscope with an accelerating voltage of 10 kV. AFM images were recorded using Agilent AFM with Pico plus molecular imaging system in the semi-contact mode. The oscillation frequency was set to approximately 255 kHz with Si cantilever which had a spring constant of about 11.5 N m^{-1}. All AFM images were undertaken at room temperature.

2.6. Ionic conductivity

The resistance value of the membranes was measured over the frequency range from 1 Hz to 1 MHz by four-point probe alternating current (AC) impedance spectroscopy using an electrode system connected with an electrochemical workstation (Zahner IM6 EX). All the samples were fully hydrated in N_2 saturated deionized water for at least 24 h prior to the conductivity measurement. Conductivity measurements under fully hydrated conditions were carried out in a chamber filled with a N_2 saturated deionized water. All the samples were equilibrated for at least 30 min at a given temperature. Repeated measurements were taken with 10 min interval until no more change in conductivity was observed. The ionic conductivity σ (S cm^{-1}) of a given membrane can be calculated from:

$$\sigma = \frac{l}{RA}$$

where l is the distance (cm) between two stainless steel electrodes, A is the cross-sectional area (cm^2) of the membrane, obtained from the membrane thickness multiplied by its width, and R is the membrane resistance value from the AC impedance data (Ω).

2.7. Water uptake and swelling ratio

The membrane samples were soaked in the N_2 saturated deionized water at room temperature for 24 h. The hydrated membranes were taken out, and the excess water on the surface was removed by wiping with a tissue paper and weighed immediately (W_w). Then the wet membrane was dried under vacuum at a fixed temperature of 80 °C until a constant dry weight was obtained (W_d). The water uptake W was calculated with the following equation:

$$W(\%) = \frac{(W_w - W_d)}{W_d} \times 100\%$$

where W_d and W_w are the mass of the dry and water-swollen samples, respectively.

The swelling ratio was characterized by linear expansion ratio (LER), which was determined by the difference between wet and dry dimensions of a membrane sample (3 cm in length and 1 cm in width). The calculation was based on the following equation:

$$\text{swelling}(\%) = \frac{X_{wet} - X_{dry}}{X_{dry}} \times 100\%$$

where X_{wet} and X_{dry} are the lengths of wet and dry membranes, respectively.

2.8. Ion exchange capacity (IEC)

Ion exchange capacities (IEC) were determined by a back-titration. The AEMs were immersed in 100 mL of 0.01 M HCl standard solution for 24 h. The solutions were then titrated with a standardized NaOH solution using phenolphthalein as an indicator. The IEC value was calculated using the expression:

$$\text{IEC} = \frac{V_{0,NaOH}C_{NaOH} - V_{x,NaOH}C_{NaOH}}{m_{dry}}$$

where $V_{0,NaOH}$ and $V_{x,NaOH}$ are the volume of the NaOH consumed in the titration without and with membranes, respectively, C_{NaOH} is the mol concentration of the NaOH, which are titrated by the standard oxalic acid solution and m_{dry} is the mass of the dry membranes. Three replicates were conducted for each sample.

2.9. Membrane stability in alkaline solution

The stability of the membranes in alkaline solution was examined by immersing the membrane samples in N_2 saturated 1 M KOH solution at 60 °C. The degradation of polymer membranes is evaluated by measuring the changes of hydroxide conductivity and IEC values.

3. Results and discussion

3.1. Synthesis of [DAMIm][Br]

In the present work, 1,3-diallyl-2-methyl imidazolium bromine ([DAMIm][Br]) was synthesized and used both as crosslinker and hydrophilic phase. [DAMIm][Br] was obtained by the reaction of 1-allyl-2-methylimidazole and an equivalent molar amount of 3-bromo-1-propene at room temperature under nitrogen atmosphere. The purity and chemical structure of the synthesized [DAMIm][Br] were confirmed by ^{1}H NMR measurements (Fig. 1). Fig. 1 exhibits the expected chemical shifts and intensities for a pure [DAMIm][Br]. Chemical shifts of the imidazolium groups are observed at 7.35 and 2.52 ppm. The chemical shifts at 5.90–6.00, 5.32–5.34 and 5.09–5.14 ppm are attributed to the allyl groups.

3.2. Preparation of imidazolium-based membranes

Scheme 1 shows the synthetic procedure for the cross-linked vinyl polymer-based anion exchange membranes. The purity and chemical structure of the imidazolium-based crosslinker which contains two unsaturated carbon–carbon bond ([DAMIm][Br]) were confirmed by ^{1}H NMR. The cross-linked membranes were

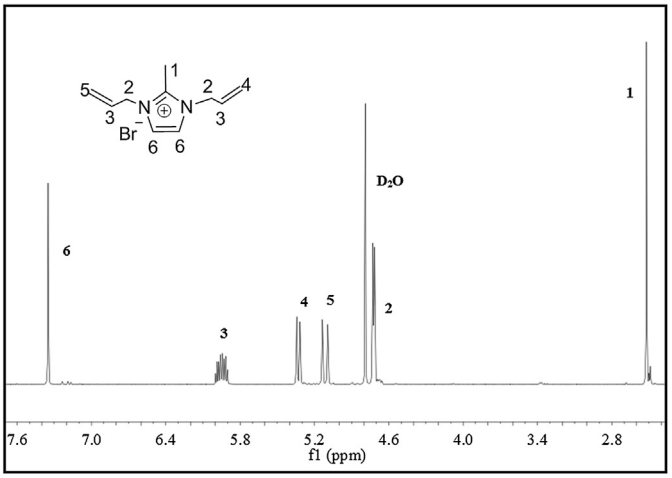

Fig. 1. ^{1}H NMR spectra of [DAMIm][Br].

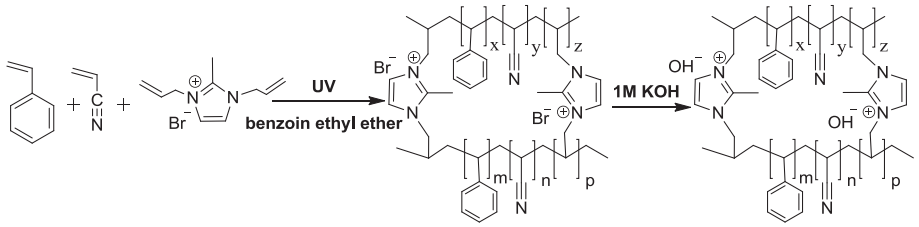

Scheme 1. General synthesis procedures for the preparation of imidazolium-based membranes.

prepared via photo-cross-linking of a mixture containing [DAMIm][Br] (10–30 wt%), styrene/acrylonitrile (1:3 weight ratio, 90–70 wt %), and benzoin ethyl ether (1 wt% based on the weight of monomer) in a glass mold. The produced cross-linked AEMs in Br^- form were denoted as $PSAN_x$-[DAMIm][Br]$_y$, and the subscript x and y indicates the weight ratio of styrene/acrylonitrile and [DAMIm][Br], respectively.

3.3. FT-IR spectra

Fig. 2 shows the Fourier transform infrared (FT-IR) spectra of the $PSAN_x$-[DAMIm][Br]$_y$ membranes. All of the membranes show the absorption bands of the cyano groups (C≡N) at 2238 cm^{-1}. The peaks at 3030–3063 and 1450–1600 cm^{-1} confirm the existence of polystyrene, and the absorption bands present at about 2970 cm^{-1} correspond to the stretching of methylene and methyl. Absorption peaks at ~1602 cm^{-1} and ~765 cm^{-1} arise from the vibrational mode of imidazolium cations, and the characteristic absorption peak of imidazolium cations increases with the increases of the concentrations of [DAMIm][Br]. The results of FT-IR confirm the chemical structure of the membranes.

The resultant AEMs in OH^- form were obtained by immersing $PSAN_x$-[DAMIm][Br]$_y$ in a N_2 saturated 1 M KOH solution for 24 h (Scheme 1), and the membranes of OH^- form were denoted as $PSAN_x$-[DAMIm][OH]$_y$. As shown in Fig. 3 the prepared $PSAN_x$-[DAMIm][OH]$_y$ are transparent, flexible, and can be easily cut into any desired sizes.

3.4. Thermal analysis

The thermal stability of the AEMs is very important for AEMFCs, because the reaction kinetics at both electrodes could be enhanced and the thermodynamic voltage losses could be reduced at a high temperature. Fig. 4 shows the typical thermogravimetric analyzer (TGA) curves of the produced AEMs in OH^- forms, which were recorded under a nitrogen flow from 30 to 600 °C at a heating rate of 10 °C min^{-1} to assess their short-term thermal stabilities. All the membranes show a slight weight loss (about 4 wt%) below 120 °C, corresponding to the evaporation of absorbed water. The weight loss region at temperatures above 300 °C due to the degradation of imidazolium cations and the backbone of copolymers. These results confirm that this type of cross-linked membranes indeed confers a high thermal stability, far beyond the range of interest for application in AEMFCs [31].

3.5. Mechanical properties

AEMs must have sufficient mechanical strength if they are to be used in the application of AEMFCs. Table 1 summarizes the mechanical properties of $PSAN_x$-[DAMIm][OH]$_y$ membranes measured at room temperature. The tensile strength of all the membranes is in the range of 14.3–30.6 MPa, with the tensile modulus of 621–1235 MPa, and the values of elongation at break of 31.1–89.8%. Commonly, chemical cross-linking is an effective method to improve the mechanical properties of the polymer membranes. However, [DAMIm][Br] used in the present work not only as a crosslinker, but also used as a hydrophilic phase. The hydrophilic phase of the membranes increased with the [DAMIm][Br] content. Therefore, $PSAN_{80}$-[DAMIm][OH]$_{20}$ showed lower tensile strength and tensile modulus than that of $PSAN_{90}$-[DAMIm][OH]$_{10}$. However, the tensile modulus of the membranes was increased from 621 to 689 Mpa when the content of [DAMIm][Br] was increased from 20 to 30 wt%, which indicating the mechanical properties of the cross-linked membranes were improved. The mechanical properties of produced cross-linked AEMs in the present work are almost equivalent to those of quaternary ammonia poly(arylene ether

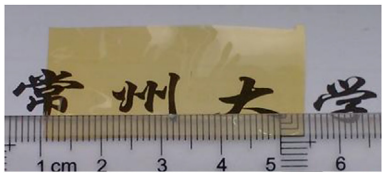

Fig. 3. Photographs of the $PSAN_{70}$-[DAMIm][OH]$_{30}$ membrane with the thickness of ~60 μm.

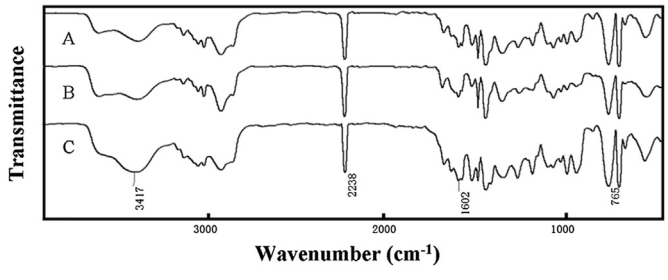

Fig. 2. FT-IR spectra of (A) $PSAN_{90}$-[DAMIm][Br]$_{10}$, (B) $PSAN_{80}$-[DAMIm][Br]$_{20}$ and (C) $PSAN_{70}$-[DAMIm][Br]$_{30}$.

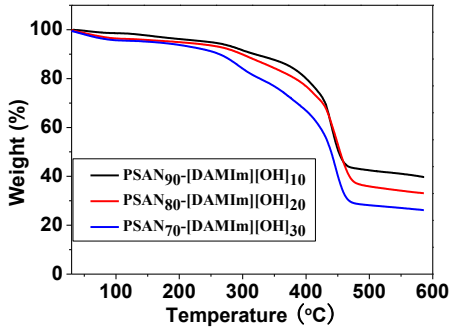

Fig. 4. TGA curves of membranes under nitrogen flow. Heating rate: 10 °C min^{-1}.

Table 1
Mechanical properties of the $PSAN_x$-[DAMIm][OH]$_y$ membranes.

Sample	Tensile strength (MPa)	Tensile modulus (MPa)	Elongation at break (%)
$PSAN_{90}$-[DAMIm][OH]$_{10}$	30.6	1235.2	31.1
$PSAN_{80}$-[DAMIm][OH]$_{20}$	14.3	621.8	89.8
$PSAN_{70}$-[DAMIm][OH]$_{30}$	16.8	689.2	76.7

sulfone)s [44]. The results indicate that the cross-linked AEMs should be tough enough for potential use as the AEM materials in AEMFC applications.

3.6. IEC, water uptake and swelling degree

It has been previously demonstrated that the ion exchange capacity (IEC) value is closely related to water uptake, swelling degree, and ionic conductivity [31–33]. Therefore, AEMs with different theoretical IEC values were synthesized by adjusting the content of [DAMIm][Br] for comparison. The values of IEC, swelling degree, water uptake, and ionic conductivity of $PSAN_x$-[DAMIm][OH]$_y$ were showed in Table 2. It is well known that the presence of water in the membrane favors the ionic conductivity of membranes. However, high water uptake usually resulted in a loss of mechanical properties. From Table 2, it could be seen that the IEC values of the produced membranes are calculated from 0.31 to 1.26 meq g^{-1}, which matched the theoretical values (0.41–1.31 meq g^{-1}) very well. The swelling behavior of the membrane is an essential factor influencing the mechanical properties and the morphologic stability of membranes. Generally, the water uptake and swelling degree increase with the IEC values. As expected, the water uptake and swelling degree of $PSAN_{90}$-[DAMIm][OH]$_{10}$ are 8.58% and 2.36% in the present work, and increased to 95.77% and 32.41% for $PSAN_{70}$-[DAMIm][OH]$_{30}$, respectively.

3.7. Ionic conductivity

The ionic conductivity of the AEMs is of particular importance and plays a significant role in AEMFCs performance. The IEC values link to the density of ionizable functional group in the membranes, and the hydrophilic properties of the membrane increased with increasing the IEC values, so it has significantly influenced on ionic conductivity of AEMs. Here, the ionic conductivity of the AEMs was measured after the membranes were fully hydrated in deionized water at room temperature. Fig. 5 shows the temperature dependence of ionic conductivity of $PSAN_x$-[DAMIm][OH]$_y$ membranes with different IEC values. For the $PSAN_x$-[DAMIm][OH]$_y$ membranes, the ionic conductivities of the AEMs at a given temperature were increased with the increasing IEC due to the increased concentration of active sites of anion transport [45] and the volume fraction of water in the membrane matrix [46]. Similar to the water uptake and swelling degree of the AEMs, $PSAN_{70}$-[DAMIm][OH]$_{30}$ with highest IEC showed the highest ionic conductivity. Besides, the conductivities of the membranes increase as temperature

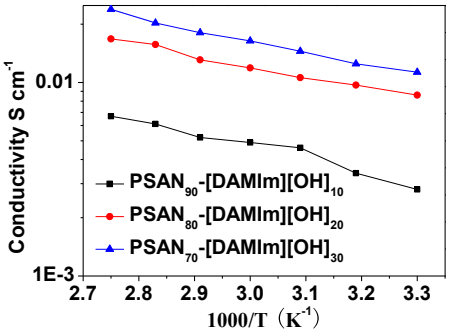

Fig. 5. Conductivity Arrhenius plots of $PSAN_x$-[DAMIm][OH]$_y$ as a function of temperature.

increases because the free volume in favor of ion transport and the mobility of anions is increased at high temperature. The conductivities of the AEMs displayed an approximate Arrhenius-type temperature dependence from 30 to 90 °C, and the apparent activation energy was 10.10–12.84 kJ mol^{-1}. These values were comparable to that of the reported AEMs [16] and the values of Nafion-117 [33].

3.8. Morphology

Note that there are dramatic property differences between $PSAN_{90}$-[DAMIm][OH]$_{10}$ and other membranes (see Tables 1 and 2). In order to interpret the differences, the morphology of the AEMs was studied using AFM. Fig. 6 shows the phase images (Fig. 6A and B) and height images (Fig. 6C and D) of $PSAN_{90}$-[DAMIm][OH]$_{10}$ and $PSAN_{70}$-[DAMIm][OH]$_{30}$. The AEMs were obtained via the polymerization of monomers in a glass mold (see the Experimental section), and the surface of glass mold is not absolutely smooth. Therefore, it is not surprising to see the rough surfaces of AEMs from the AFM height images (Fig. 6C and D). Changes in the phase images reflect changes of surface roughness, composition, hardness, friction, viscoelasticity and etc. The minimal correlation between phase images and height images indicates that phase images are unlikely to be an artifact of surface roughness. From the AFM phase images, the dark regions increase with increasing the [DAMIm][OH] content of AEMs. Therefore, the brighter regions are hard polymer domains which correspond to hydrophobic regions, while the dark regions correspond to the soft polymer domains which correspond to hydrophilic charged imidazole groups [47,48]. There is a morphological transition of the hydrophilic domains from isolated to continuous with the increase of [DAMIm][OH] content, which can be found from the AFM phase images (Fig. 6A, B). The continuous hydrophilic polymeric networks formed within the membranes significantly affect the ionic conductivity of the membranes. We believe that such a homogeneously distribution and continuous hydrophilic domains favor the formation of the ion

Table 2
Ion exchange capacity (IEC), water uptake, swelling degree, and conductivity of $PSAN_x$-[DAMIm][OH]$_y$ membranes.

Sample	IEC (meq g^{-1})		Water uptake (%)[b]	Swelling degree (%)[b]	Conductivity ($\times 10^{-2}$ S cm^{-1})	
	Theoretical[a]	Experimental			30 °C	60 °C
$PSAN_{90}$-[DAMIm][Br]$_{10}$	0.41	0.31 ± 0.04	8.58	2.36	0.28 ± 0.03	0.49 ± 0.08
$PSAN_{80}$-[DAMIm][Br]$_{20}$	0.85	0.77 ± 0.07	86.56	23.94	0.86 ± 0.09	1.19 ± 0.21
$PSAN_{70}$-[DAMIm][Br]$_{30}$	1.31	1.22 ± 0.06	95.77	32.41	1.13 ± 0.11	1.64 ± 0.19

[a] Calculated from monomer ratio.
[b] After immersing in water at RT for 24 h average of two trials.

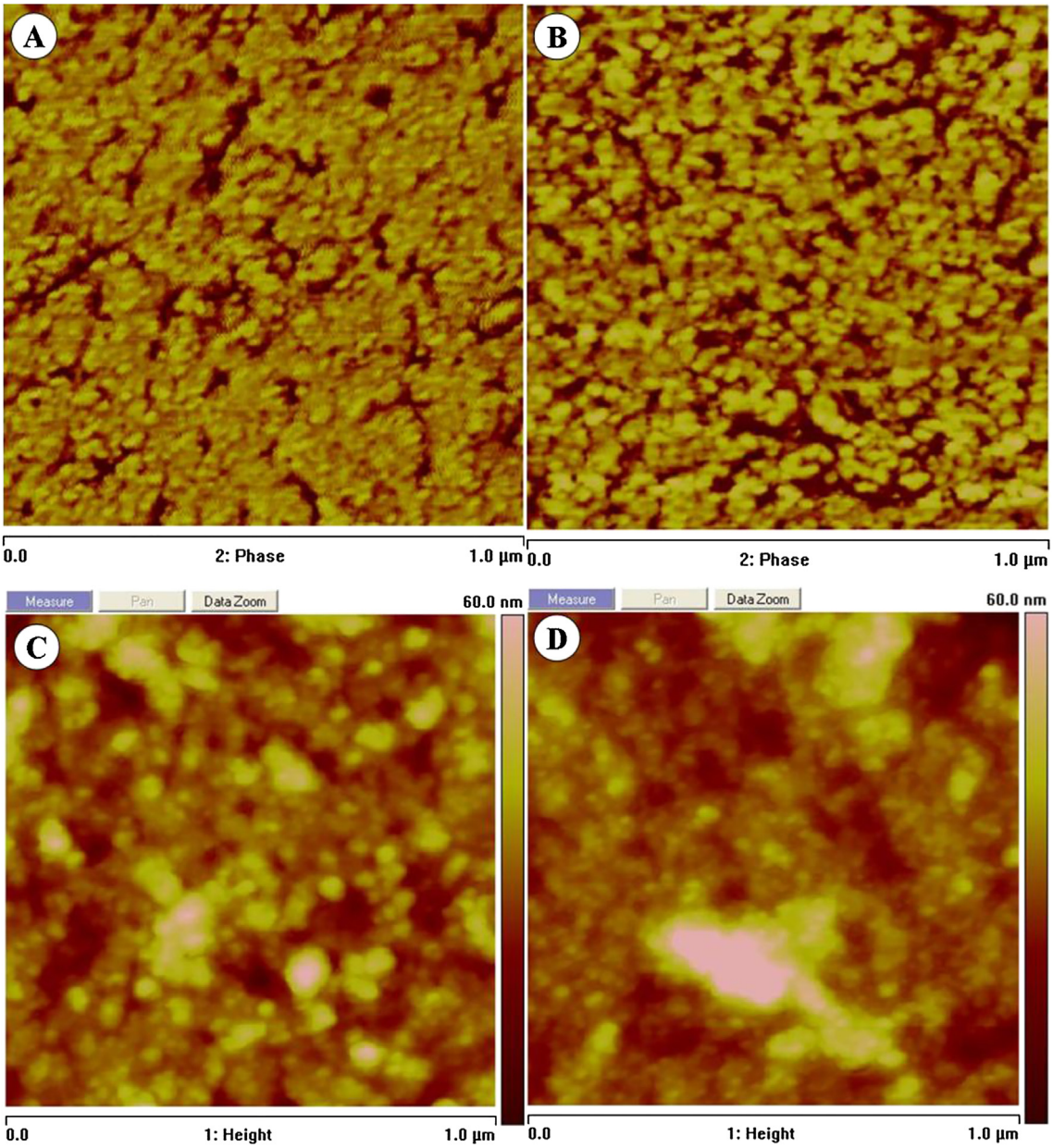

Fig. 6. AFM phase images (A, B) and height images (C, D) of $PSAN_{90}$-[DAMIm][OH]$_{10}$ (A, C) $PSAN_{70}$-[DAMIm][OH]$_{30}$ (B, D).

transport channel, which therefore enhance the conductivity of the AEMs.

3.9. Alkaline stability

From the viewpoint of applications, a major concern in AEMs is the chemical stability, especially the stability in alkaline media at elevated temperature. Here, the alkaline stability of $PSAN_x$-[DAMIm][OH]$_y$ was investigated by immersing the samples into 1 M KOH solution at 60 °C to check the changes of IEC values and ionic conductivity of the samples. Fig. 7 shows the ionic conductivity of $PSAN_{70}$-[DAMIm][OH]$_{30}$ after treatment with N_2 saturated 1 M KOH solution at 60 °C for different times. No obvious changes of the conductivity could be observed from Fig. 7, which indicating an excellent alkaline stability of $PSAN_{70}$-[DAMIm][OH]$_{30}$ in KOH solution. The IEC values of $PSAN_{70}$-[DAMIm][OH]$_{30}$ also kept constant during the stability test in 1 M KOH solution, further confirming

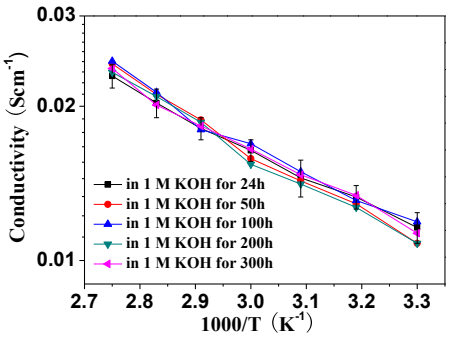

Fig. 7. Conductivity Arrhenius plots of $PSAN_{70}$-[DAMIm][OH]$_{30}$ after immersion in N_2 saturated 1 M KOH solution at 60 °C for various times.

Table 3
The ion exchange capacity (IEC) values of N_{70}-[DAMIm][OH]$_{30}$ membranes be immersed in 1 M KOH solution at 60 °C.

Time immersed in 1 M KOH (h)	IEC (meq g^{-1})
0	1.22 ± 0.06
24	1.26 ± 0.05
50	1.24 ± 0.07
100	1.25 ± 0.07
200	1.24 ± 0.06
300	1.24 ± 0.04

good chemical stability of the membranes in alkaline solution (Table 3). The excellent alkaline stability of PSAN$_x$-[DAMIm][OH]$_y$ is due to two reasons: (i) the resonance effect of the conjugated imidazole rings reduce the positive charge density of the imidazolium cation, and thus improve the imidazolium-based cross-linked AEMs; (ii) the electron density of imidazolium cations could be increased by hyperconjugative effect between the C–H (σ bond) of methyl group and the π-conjugated imidazole ring, which thus further enhances the alkaline stability of AEMs.

4. Conclusions

In summary, we have demonstrated a facile and effective synthetic procedure for the preparation of novel cross-linked vinyl polymer-based AEMs. The AEMs were prepared via irradiation with ultraviolet light cross-linking of styrene, acrylonitrile and [DAMIm][Br], and followed by anion exchange with hydroxide ions. [DAMIm][Br] was used both as crosslinker and ionic conductor (hydrophilic phase). The resultant membranes are flexible and tough enough for potential use as AEMs for AEMFC applications. The thin films contained [DAMIm][Br] with a mass fraction of 30% exhibit hydroxide conductivity above 10^{-2} S cm^{-1} and the good chemical stability in high pH solution at 60 °C, indicating that the membranes fulfill the basic require of AEMFCs. The results of this study suggest a feasible approach for the synthesis and practical applications of alkaline AEMs, and should be expected to promote the widespread use of AEMFCs.

Acknowledgment

This work was supported by National Natural Science Foundation of China (_501100001809) (Nos. 51303017, 51272033, 51342010 and 21301021).

References

[1] M.Z. Jacobson, W.G. Colella, D.M. Golden, Science 308 (2005) 1901–1905.
[2] B.C.H. Steele, A. Heinzel, Nature 414 (2001) 345–352.
[3] K.A. Mauritz, R.B. Moore, Chem. Rev. 104 (2004) 4535–4585.
[4] M.A. Hickner, H. Ghassem, Y.S. Kim, B.R. Einsla, J.E. McGrath, Chem. Rev. 104 (2004) 4587–4612.
[5] C. Zhao, Y. Gong, Q. Liu, Q. Zhang, A. Zhu, Int. J. Hydrogen Energy 37 (2012) 11383–11393.
[6] H. Sun, G. Zhang, Z. Liu, N. Zhang, L. Zhang, W. Ma, C. Zhao, D. Qi, G. Li, H. Na, Int. J. Hydrogen Energy 37 (2012) 9873–9881.
[7] K. Miyatake, T. Shimura, T. Mikamiac, M. Watanabe, Chem. Commun. 42 (2009) 6403–6405.
[8] M.S. Whittingham, R.F. Savinelli, T.A. Zawodzinski, Chem. Rev. 104 (2004) 4243–4244.
[9] K. Yasuda, A. Taniguchi, T. Akita, T. Ioroi, Z. Siroma, Phys. Chem. Chem. Phys. 8 (2006) 746–752.
[10] S. Lu, J. Pan, A. Huang, L. Zhuang, J. Lu, Proc. Natl. Acad. Sci. USA 105 (2008) 20611–20614.
[11] M. Ünlü, J. Zhou, P.A. Kohl, Angew. Chem. Int. Ed. 49 (2010) 1299–1301.
[12] B. Lin, S. Cheng, L. Qiu, F. Yan, S. Shang, J. Lu, Chem. Mater. 22 (2010) 1807–1813.
[13] J. Wang, Z. Zhao, F. Gong, S. Li, S. Zhang, Macromolecules 42 (2009) 8711–8717.
[14] Y. Leng, G. Chen, A.J. Mendoza, T.B. Tighe, M.A. Hickner, C. Wang, J. Am. Chem. Soc. 134 (2012) 9054–9057.
[15] Y. Wu, C. Wu, J.R. Varcoec, S.D. Poynton, T. Xu, Y. Fu, J. Power Sources 195 (2010) 3069–3076.
[16] J. Pan, S. Lu, Y. Li, A. Huang, L. Zhuang, J. Lu, Adv. Funct. Mater. 20 (2010) 312–319.
[17] G. Wang, Y. Weng, D. Chu, D. Xie, R. Chen, J. Membr. Sci. 326 (2009) 4–8.
[18] M. Zhang, H.K. Kim, E. Chalkova, F. Mark, S.N. Lvov, T.C.M. Chung, Macromolecules 44 (2011) 5937–5946.
[19] Q. Zhang, S. Li, S. Zhang, Chem. Commun. 46 (2010) 7495–7497.
[20] D.S. Kim, A. Labouriau, M.D. Guiver, Y.S. Kim, Chem. Mater. 23 (2011) 3795–3797.
[21] C. Qu, H. Zhang, F. Zhang, B. Liu, J. Mater. Chem. 22 (2012) 8203–8207.
[22] S. Gu, R. Cai, T. Luo, Z. Chen, M. Sun, Y. Liu, G. He, Y. Yan, Angew. Chem. Int. Ed. 48 (2009) 6499–6502.
[23] S. Gu, R. Cai, Y. Yan, Chem. Commun. 47 (2011) 2856–2858.
[24] K.J.T. Noonan, K.M. Hugar, H.A. Kostalik, E.B. Lobkovsky, H.D. Abruña, G.W. Coates, J. Am. Chem. Soc. 134 (2012) 18161–18164.
[25] C.G. Arges, J. Parrondo, G. Johnson, A. Nadhan, V.J. Ramani, J. Mater. Chem. 22 (2012) 3733–3744.
[26] J. Ran, L. Wu, J.R. Varcoe, A.L. Ong, S.D. Poynton, T. Xu, J. Membr. Sci. 415-416 (2012) 242–249.
[27] Q. Hu, Y. Shang, Y. Wang, M. Xu, W. Wang, X. Xie, S. Wang, H. Zhang, J. Wang, Z. Mao, Int. J. Hydrogen Energy 37 (2012) 12659–12665.
[28] B. Lin, L. Qiu, B. Qiu, Y. Peng, F. Yan, Macromolecules 44 (2011) 9642–9649.
[29] W. Li, J. Fang, M. Lv, C. Chen, X. Chi, Y. Yang, Y. Zhang, J. Mater. Chem. 21 (2011) 11340–11346.
[30] X. Yan, G. He, S. Gu, X. Wu, L. Du, Y. Wang, Int. J. Hydrogen Energy 37 (2012) 5216–5224.
[31] B. Qiu, B. Lin, L. Qiu, F. Yan, J. Mater. Chem. 22 (2012) 1040–1045.
[32] M. Guo, J. Fang, H. Xu, W. Li, X. Lu, C. Lan, K. Li, J. Membr. Sci. 362 (2010) 97–104.
[33] B. Lin, L. Qiu, J. Lu, F. Yan, Chem. Mater. 22 (2010) 6718–6725.
[34] F. Zhang, H. Zhang, C. Qu, J. Mater. Chem. 21 (2011) 12744–12752.
[35] B. Qiu, B. Lin, Z. Si, L. Qiu, F. Chu, J. Zhao, F. Yan, J. Power Sources 217 (2012) 329–335.
[36] D. Chen, M.A. Hickner, ACS Appl. Mater. Interfaces 4 (2012) 5775–5781.
[37] O.D. Thomas, K.J. Soo, T.J. Peckham, M.P. Kulkarni, S. Holdcroft, J. Am. Chem. Soc. 134 (2012) 10753–10756.
[38] D. Henkensmeier, H.J. Kim, H.J. Lee, D.H. Lee, I.H. Oh, S.A. Hong, S.W. Nam, T.H. Lim, Macromol. Mater. Eng. 296 (2011) 899–908.
[39] D. Henkensmeier, H.R. Cho, H.J. Kim, C.N. Kirchner, J. Leppin, A. Dyck, J.H. Jang, E. Cho, S.W. Nam, T.H. Lim, Polym. Degrad. Stab. 97 (2012) 264–272.
[40] O.D. Thomas, K.J.W.Y. Soo, T.J. Peckham, M.P. Kulkarni, S. Holdcroft, Polym. Chem. 2 (2011) 1641–1643.
[41] B. Lin, H. Dong, Y. Li, Z. Si, F. Gu, F. Yan, Chem. Mater. 25 (2013) 1858–1867.
[42] S.A. Nuñez, M.A. Hickner, ACS Macro Lett. 2 (2013) 49–52.
[43] Y. Luo, J. Guo, C. Wang, D. Chu, J. Power Sources 195 (2010) 3765–3771.
[44] J. Wang, S. Li, S. Zhang, Macromolecules 43 (2010) 3890–3896.
[45] T.J. Peckham, J. Schmeisser, M. Rodgers, S. Holdcro, J. Mater. Chem. 17 (2007) 3255–3268.
[46] A. Siu, J. Schmeisser, S. Holdcro, J. Phys. Chem. B 110 (2006) 6072–6080.
[47] S. Yu, F. Yan, X. Zhang, J. You, P. Wu, J. Lu, Q. Xu, X. Xia, G. Ma, Macromolecules 41 (2008) 3389–3392.
[48] F. Yan, S. Yu, X. Zhang, L. Qiu, F. Chu, J. You, J. Lu, Chem. Mater. 21 (2009) 1480–1484.